

Comparison between non orographic gravity wave drag parameterizations used in QBOi models and Strateole 2 constant level balloons

F. Lott¹, R. Rani¹, C. McLandress⁴, A. Podglagen¹, A. Bushell⁵, M. Bramberger⁹, H.-K. Lee⁶, J. Alexander⁹, J. Anstey⁴, H.-Y. Chun⁶, A. Hertzog², Y.-H. Kim⁷, B. Legras¹, E. Manzini⁸, H. Naoe¹⁰, S. Osprey¹¹, R. Plougonven³, H. Pohlmann⁸, J. H. Richter¹², J. Scinocca⁴, J. Serrano¹³, F. Serva¹⁴, T. Stockdale¹⁵, S. Versick¹⁶, S. Watanabe¹⁷, K. Yoshida¹⁷

¹Laboratoire de Météorologie Dynamique (LMD)/IPSL, PSL Research Institute, Ecole Normale Supérieure, Paris, France.

²LMD/IPSL, Sorbone Université, Paris, France.

³LMD/IPSL, Ecole Polytechnique, Institut Polytechnique de Paris, Palaiseau, France

⁴Canadian Centre for Climate Modelling and Analysis (CCCma), Victoria, Canada

⁵Met Office, FitzRoy Road, Exeter, UK

⁶Yonsei University, Seoul, South Korea

⁷Institut für Atmosphäre und Umwelt, Goethe-Universität, Frankfurt am Main, Germany

⁸Max Planck Institute for Meteorology, Hamburg, Germany

⁹NorthWest Research Associates, Boulder Office, Boulder, CO, USA

¹⁰Meteorological Research Institute (MRI), Tsukuba, Japan

¹¹Atmospheric, Oceanic and Planetary Physics, University of Oxford, Oxford, UK

¹²National Center for Atmospheric Research (NCAR), Boulder, Colorado, USA

¹³Group of Meteorology Universitat de Barcelona, Barcelona, Spain

¹⁴Institute of Marine Sciences, National Research Council, Rome, Italy

¹⁵European Centre for Medium-Range Weather Forecasts (ECMWF), Reading, UK

¹⁶Karlsruher Institut für Technologie (KIT), Karlsruhe, Germany

¹⁷Japan Agency for Marine-Earth Science and Technology (JAMSTEC), Yokohama, Japa

Key Points:

- The non-orographic parameterization tuned to produce a realistic tropical quasi-biennial oscillation in global climate models are used to predict in-situ observations.
- Parameterized gravity waves needed in large-scale models have realistic amplitudes in the tropical lower stratosphere.
- Day-to-day variations of the estimated gravity wave momentum fluxes correlate in some cases with observations, except when launching level are near the tropopause.
- The probability density distribution of the parameterized momentum fluxes are better reproduced when the schemes are not related to their convective sources and/or when the launching level is in the lower and middle troposphere.

Version 1, date: December 28, 2023

Corresponding author: Francois Lott, flott@lmd.ens.fr

39
40
41
42
43
44
45
46
47
48
49
50
51
52
53
54
55
56
57
58
59
60
61
62
63
64
65**Abstract**

Gravity Waves (GWs) parameterizations from 14 General Circulation Models (GCMs) participating to the Quasi-Biennial Oscillation initiative (QBOi) are directly compared to Strateole-2 balloon observations made in the lower tropical stratosphere from November 2019 to February 2020 (phase 1) and from October 2021 and January 2022 (phase 2). The parameterizations used span the 3 state of the arts techniques used in GCMs to represent subgrid scale non-orographic GWs, the two globally spectral techniques developed by Hines (1997) and Warner and McIntyre (1999) respectively and the "multiwaves" approaches following Lindzen (1981). The input meteorological fields necessary to run the parameterizations offline are extracted from the ERA5 reanalysis and correspond to the instantaneous meteorological conditions found underneath the balloons. In general, the amplitudes are in fair agreement between measurements of the momentum fluxes due to waves with periods less than 1 hr and the parameterizations. The correlation of the daily values between the observations and the results of the parameterization can be around 0.4, which is statistically elevated considering that we analyse around 1200 days of data and sometime good considering that the parameterizations have not been tuned: the schemes used are just the standard ones that help producing a Quasi-Biennial Oscillation (QBO) in the corresponding model. These correlations nevertheless vary considerably between schemes and depend little on their formulation (globally spectral versus multiwaves for instance). We therefore attribute it to dynamical filtering all schemes taking good care of it, whereas only few relate the gravity waves to their sources. Except for one parameterization, significant correlations are mostly found for eastward propagating waves, which may be due to the fact that during both Strateole 2 phases the QBO phase is easterly at the altitude of the balloon flights. On the other hand, statistical properties, like pdf of momentum fluxes seem better represented in spectral schemes with constant sources than in schemes ("spectral" or "multiwaves") that relate GWs to their convective sources.

66

Plain Language Summary67
68
69
70
71
72
73
74
75
76
77
78
79

In most large-scale atmospheric models, gravity wave parameterizations are based on well understood but simplified theories and parameters which are keyed to reduce systematic errors on the planetary scale winds. In the equatorial regions, the most challenging errors concern the Quasi Biennial Oscillation. Although it has never been verified directly, it is expected that the parameterizations tuned this way should transport a realistic amount of momentum flux in both the eastward and westward directions when compared to direct observations. Here we show that it is the case, to a certain extent, using constant-level balloon observations at 20 km altitude. The method consists in comparing directly, each day and at the location of the balloon the measured momentum fluxes and the estimations from the gravity wave parameterizations used in the global models that participate to the Quasi-Biennial Oscillation initiative and when using observed values of the large-scale meteorological conditions of wind, temperature, precipitation, and diabatic heating.

1 Introduction

It is well known that the large scale circulation in the middle atmosphere is in good part driven by gravity waves (GWs) that propagate in the stratosphere (Andrews et al., 1987). These waves carry horizontal momentum vertically and interact with the large scale flow when they break. The horizontal scale of these waves can be quite short, much shorter than the horizontal scale of General Circulation Models (GCMs) so they need to be parameterized (Alexander & Dunkerton, 1999). In the tropics, the convective GWs are believed to dominate largely (Fovell et al., 1992; Alexander et al., 2000; Lane & Moncrieff, 2008), they contribute significantly to the forcing of the Quasi-Biennial Oscillation (QBO), a near 28-month oscillation of the zonal mean zonal winds that occurs in the lower part of the equatorial stratosphere (Baldwin et al., 2001). For these reasons, the parameterization of convective GWs is necessary for most GCMs to explicitly realize the QBO.

Although gravity wave parameterizations are now used in many models with success including in the tropics (Scinocca, 2003; Song & Chun, 2005; Beres et al., 2005; Orr et al., 2010; Lott & Guez, 2013; Bushell et al., 2015; Anstey et al., 2016; Christiansen et al., 2016; Serva et al., 2018), their validation using direct in situ observations remains a challenge. There exist observations of GWs using global satellite observations (Geller et al., 2013) but the GWs identified this way still have quite large horizontal scales, and some important quantities like the Momentum Fluxes (MFs) are often deduced indirectly, for instance from temperature measurements using polarization relations (Alexander et al., 2010; Ern et al., 2014). For these two reasons, in situ observations are essential, and the most precise ones are provided by constant-level long-duration balloons, like those made in the Antarctic region during Strateole-Vorcore (Hertzog, 2007) and Concordiasi (Rabier et al., 2010), or in the deep tropics during PreConcordiasi (Jewtoukoff et al., 2013) and Strateole 2 (Haase et al., 2018). Among many important results, these balloon observations have shown that the momentum flux entering in the stratosphere is extremely intermittent (Hertzog et al., 2012). This intermittency implies that the mean momentum flux is mostly transported by few large-amplitude waves that potentially break at lower altitudes than when the GW field is more uniform. This property, when reproduced by a parameterization (de la Cámara et al., 2014; Kang et al., 2017; Alexander et al., 2021), can help reduce systematic errors in the midlatitudes, for instance on the timing of the final warming in the Southern Hemisphere polar stratosphere (de la Cámara et al., 2016), or on the QBO (Lott et al., 2012). Balloon observations have also been used to characterize the dynamical filtering by the large scale winds (Plougonven et al., 2017), and to validate the average statistical properties of the GW momentum flux predicted offline using reanalysis data (Kang et al., 2017; Alexander et al., 2021).

However, the evaluation of parameterizations using balloon observations often done in the past were often quite indirect, and concern more their statistical behaviours (Jewtoukoff et al., 2015; Kang et al., 2017; Alexander et al., 2021) than their capacity to directly predict instantaneous values of momentum fluxes. Maybe a good reason to believe so is that parameterizations are based on simplified quasi-linear wave theory, they assume spectral distributions that are loosely constrained, and they ignore lateral propagation almost entirely (some attempt to include it can be found in Amemiya and Sato (2016)). Nevertheless, some factors could mitigate these weaknesses. One is that in most parameterizations the wave amplitude is systematically limited by a breaking criterion that encapsulates nonlinear effects. An other is that some parameterizations explicitly relate launched waves to sources, and there is constant effort to improve the realism of the convective ones (Liu et al., 2022). Also, observations systematically suggest that dynamical filtering by the large scale wind is extremely strong for upward propagating GWs (Plougonven et al., 2017), and this central property is represented in most GW parameterizations. For all these reasons, it may well be that GW parameterizations keyed to

132 the large scale conditions found at a given place and time gives MFs that can be directly
133 compared to the MFs measured by a balloon at the same place.

134 Based on the relative success of the offline calculations done in the past using re-
135 analysis data (Jewtoukoff et al., 2015; Kang et al., 2017; Alexander et al., 2021), Lott
136 et al. (2023) have shown that such a direct comparison gives result of interest. The first
137 is that a state of the art convective gravity wave drag scheme, predicts momentum fluxes
138 in the low equatorial stratosphere which amplitude can be directly compared with those
139 measured during phase 1 of the Strateole-2 balloon campaign. It gives a direct in-situ
140 observational confirmation that the theories and modelling of the QBOs developed over
141 the last 50 years were in good part correct about the significance of the GWs to the QBO
142 forcing. Also interesting, the comparison showed a good level of correlation between the
143 day to day variability in momentum fluxes between measured and observed fluxes, a cor-
144 relation that is much better for waves carrying momentum fluxes in the eastward direc-
145 tion than in the westward direction. It was suggested that such a good correlation was
146 due to the fact that the Lott and Guez (2013)’s scheme analysed relate the gravity waves
147 to their convective sources (not all schemes do) and that the GWs experience significant
148 dynamical filtering in the middle troposphere and lower stratosphere. Lott et al. (2023)
149 nevertheless revealed that a scheme that relates gravity waves to convection exclusively
150 somehow failed in predicting the right statistical behaviour of the momentum fluxes, the
151 probability density function of the momentum fluxes amplitude showing long tails for
152 low values of the MFs, suggesting missing processes like lateral propagation or the pres-
153 ence of a background of waves which origin remains a challenge to predict.

154 The purpose of this paper is to continue such a direct comparison including more
155 recent Strateole 2 observations and near all the gravity wave parameterization schemes
156 used by the modelling groups participating to the Quasi-Biennial Oscillation initiative
157 (QBOi, Butchart et al., 2018). We will follow for that Lott et al. (2023) and use the 8
158 balloons of the first phase of the Strateole 2 campaign that flew in the lower tropical strato-
159 sphere between November 2019 and February 2020 and extent it to the 15 balloons that
160 flew more than one day during the second phase of the Strateole 2 campaign, between
161 October 2021 and January 2022. For each of the flights and each time, we have identi-
162 fied the grid point in the ERA5 reanalysis (Hersbach et al., 2020) that is the nearest and
163 used the vertical profiles of wind and temperature as well as the surface value of precip-
164 itation to emulate the parameterization of GWs used in the global models that partic-
165 ipated to the Quasi-Biennial Oscillation initiative (QBOi). We also extract from the anal-
166 ysis and short range forecast, diabatic heatings and the cloud base and top altitudes needed
167 in some schemes to predict gravity waves.

168 2 Data and method

169 2.1 Parameterizations of non orographic gravity wave schemes

170 The parameterizations schemes used to predict orographic gravity waves belongs
171 to two well separated families, dating back from the 1980’s when it becomes evident that
172 a good simulation of the middle atmosphere by global atmospheric models could not be
173 done without taking into account non-orographic gravity waves. The first family roots
174 in the formulation by Lindzen (1981), where the gravity wave field is represented by grav-
175 ity waves that are monochromatic in the horizontal space and time. It was extended to
176 treat a large ensemble of waves by Alexander and Dunkerton (1999) making the assump-
177 tion that the breaking of each waves could be made independent from the others. An
178 advantage of such schemes is that it roots in linear theories where sources like convec-
179 tion and/or fronts can be introduced using closed form theories (Beres et al., 2005; Song
180 & Chun, 2005; Richter et al., 2010; Lott & Guez, 2013; de la Cámara & Lott, 2015). In
181 the following we will refer to such schemes as ”multiwave”, they are expensive because
182 they request a large amount of waves to represent well a realistic wave field, but this limit

	p_l	F_{LT}	$2\pi/m_*$	C_{\min}
CMAM	100hPa	1.3mPa	1km	0.25 m/s
IFS	450hPa	5mPa	3km	0.5 m/s
ECEarth	450hPa	3.75mPa	2km	0.25 m/s
UKMO	1000hPa	Precip	4.3km	?

Table 1. WMI Parameters changing between CMAM, IFS, ECEarth, and UKMO. UKMO is shown distinctly because it is based on (Warner & McIntyre, 1999) simplified version of WMI rather than on (Scinocca, 2003)’s and realte launched MF to precipitations.

183 can easily be circumvented by using stochastic approaches (Eckermann, 2011; Lott et
184 al., 2012). As an alternative, but also to better represent breaking, many centers devel-
185 oped globally spectral schemes. These schemes uses the observational fact that in ob-
186 servations the vertical shape of the spectra have a quite universal character. In the early
187 1990’s Hines (1991) developed a theory where GW breaking is represented by imposing
188 an upper limit to the range of vertical wavenumber, the limit being calculated accord-
189 ing to the large scale wind and including a Doppler spreading by the other gravity waves
190 (see also Hines, 1997). The scheme has been implemented with success in various GCMs
191 (see for instance Manzini, McFarlane, & McLandress, 1997), and will be referred to as
192 ”HDS” in the following. As an alternative, the theory in Warner and McIntyre (1996)
193 imposes gravity wave saturation according to an empirical spectra but treat vertical changes
194 in the spectra following GWs propagation invariant character. The theory has been sim-
195 plified and/or optimized to permit implementation, for instance in the UKMO model (Warner
196 & McIntyre, 1999; Scaife et al., 2002) and in the CMAM model (Scinocca, 2003) respec-
197 tively, and will be refered to has ”WMI” in the following. To a certain extent, the spec-
198 tral schemes can also take into account the relation with sources, for instance the HDS
199 scheme has been related to fronts in (Charron & Manzini, 2002), and the UKMO ver-
200 sion of the WMI scheme to precipitations in (Bushell et al., 2015).

201 In the present paper, we are going to compare the GWs schemes used in 14 of the
202 models that participate to QBOi, all belonging to one of the three type of schemes de-
203 scribed above (WMI, HDS, and Multiwave). As all the multiwave schemes used relate
204 GWs to their convective sources and as only one of the spectral scheme is doing so, the
205 UKMOgws WMI scheme in (Bushell et al., 2015), the former will be discussed with the
206 source-related multiwave schemes.

207 Among the 14 models, three use the (Scinocca, 2003)’s version of the WMI: CMAM,
208 IFS and ECEarth. Their version for QBOi and further detailed in (Anstey et al., 2016;
209 Orr et al., 2010; Davini et al., 2017), they essentially differ by four parameters, the launch
210 level pressure p_l , the launched momentum flux F_{LT} , the characteristic vertical wavenum-
211 ber m_* and a minimum intrinsic phase speed in the launched spectra, the values of each
212 being given here in Table 2.1. Note that for EC-Earth the exact value of the paramet-
213 ers in Table 2.1 are from J. Garcia Serrano (private communication).

214 Still among the 14 models, 5 uses the (Hines, 1997)’s parameterization schemes pre-
215 sented in (Manzini et al., 1997). Between the five models, and in the Hines scheme, only
216 changes between models the launching level p_l , the root mean square of the horizontal
217 wind variability due to GWs at launch level σ , as well as an effective horizontal wavenum-
218 ber K^* . There are also more numerical parameters that eventually changes, a minimum
219 value for the the cutoff vertical wavenumber m_{\min} , and two parameters that control smooth-
220 ing in the vertical of the GWs root mean square variance and cut-off vertical wavenum-

	p_l	σ_s	$2\pi/K^*$	m_{\min}	C_{smo}	N_{smo}
ECham5	450hPa	1.	125km	0	2	5
MIROC	650hPa	0.95	250km	$6.5 \cdot 10^{-5}$	2	2
MPIM	650hPa	1.2	125km	0	2	2
MRI-ESM	700hPa	1.9	1250km	$3.3 \cdot 10^{-4}$	4	2
EMAC	650hPa	1.	125km	0	2	2

Table 2. HDS Parameters changing between ECHam5, MIROC, MPIM, MRI-ESM, and EMAC.

	p_l	Phase Speed	Δz	Source
LMDz	500hPa	-30m/s<Intrinsic<30m/s	1km	Precip
Yonsei	900hPa-100hPa	-100m/s<Absolute<100m/s	100m-15km	Heating rate
WACCM	?			Heating rate

Table 3. Some parameters changing between LMDz, YONSEI and WACCM, for information only the schemes being extremely distinct

221 ber, the coefficient C_{smo} and the number of time the smoothing is applied N_{smo} (see
 222 Table 2.1).

223 Finally the last 4 schemes we consider all links GWs to sources (convection or precipi-
 224 tation), 3 are multiwaves and have been developed independently one from the oth-
 225 ers, LMDz, YONSEI, and WACCM and 1 uses the ultra simple version of the WMI schemes
 226 presented in (Warner & McIntyre, 1999; Bushell et al., 2015) rather than the (Scinocca,
 227 2003)’s version. The differences between the 3 multiwave schemes are numerous it is im-
 228 possible to details them, the reader is referred to the corresponding papers. The most
 229 salient differences are in the source term, the launching levels and the intrinsic phase speed
 230 of the launched waves. In LMDz is made the choice to relate the launched MF to square
 231 precipitation P_r^2 consistent with linear theory before breaking (Lott & Guez, 2013) whereas
 232 in (Bushell et al., 2015) it is related to $\sqrt{P_r}$ (see Table 2.1). Still in LMDz, the waves
 233 are launched from the mid troposphere, whereas they are launched from the surface in the
 234 UKMOgws model. In the Yonsei’s and WACCM scheme (Song & Chun, 2005; Choi &
 235 Chun, 2011), the launched momentum flux is directly related to convective heating dis-
 236 tributed in the vertical between the cloud bottom and cloud top, the launch altitude be-
 237 ing at the cloud top. In this case the launching level can vary between $2km$ and $15km$
 238 typically and the depth of the heating between $100m$ and $15km$. Also, the absolute phase
 239 speed cover the ranges $100m/s < C_{abs} < 100m/s$.

240 **2.2 Offline parameterization runs**

241 To activate the schemes in offline mode we will use ERA-5 hourly data of precipi-
 242 tation and 3-hourly data of winds, surface pressure, temperature, cloud liquid and ice
 243 water content at $1^\circ \times 1^\circ$ horizontal grid to mimic a large scale climate model resolution.
 244 Winds, surface pressure, temperature, and water contents are then linearly interpolated
 245 on 1hr time step to be synchronised with precipitation. In the vertical we use data at
 246 67 model levels, taking one every two ERA5 levels again to mimic large scale models ver-
 247 tical resolution but also to speed up calculations. To estimate convective heating rates
 248 vertical profiles, we follow (Fueglistaler et al., 2009) and evaluate diabatic heating us-

249 ing ERA5 hourly data from short range forecast and as a residual between the param-
 250 eterized temperature tendency and the radiative heatings (longwave plus shortwave). When
 251 needed, we also evaluate the cloud bottom height and top height using the cloud water
 252 content (liquid+ice) from ERA5 reanalysis.

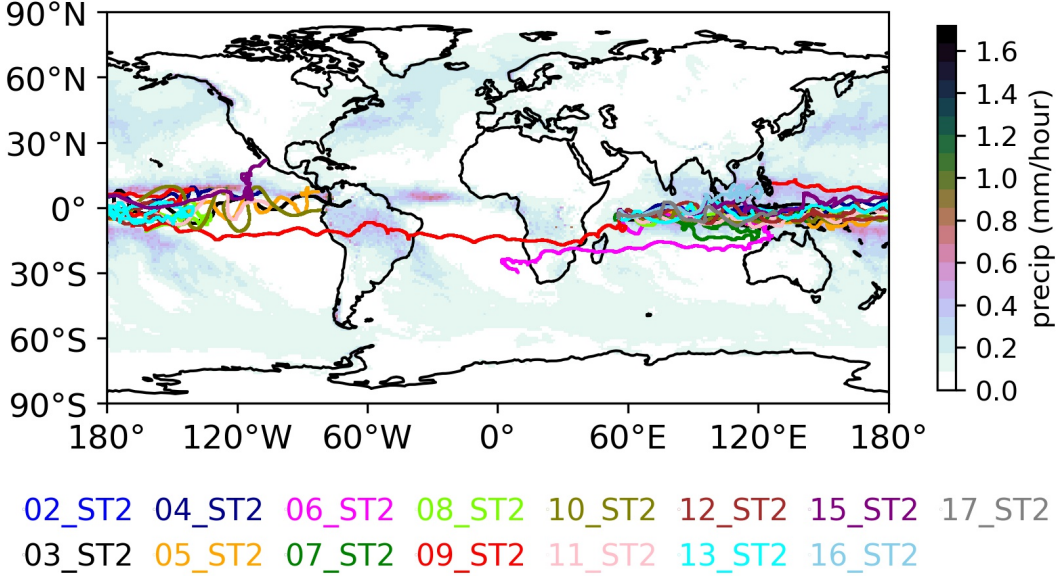


Figure 1. Strateole 2, Phase 2 balloon trajectories taking place between October 2021 and January 2022. Shading presents the precipitation field from ERA5 averaged over the period.

253 **2.3 Strateole 2 balloon observations**

254 The in situ observations we use are from the 8 balloons of the first phase of the Stra-
 255 teole 2 campaign that flew in the lower tropical stratosphere between November 2019
 256 and February 2020 and from the 15 balloons that flew more than one day during the sec-
 257 ond phase of the Strateole 2 campaign, between October 2021 and January 2022. The
 258 trajectories during phase 2 are shown in Figure 1, superimposed upon the averaged pre-
 259 cipitation (the same Figure but for phase 1 is in Lott et al. (2023)). In the MFs calcu-
 260 lated from observations Corcos et al. (2021) distinguish the waves with short periods (1hr-
 261 15mn) from the waves with period up to one day (1d-15mn). They also distinguish the
 262 eastward waves giving positive MF in the zonal direction from the westward waves giv-
 263 ing negative MF. It is important to notice that during phase 2, the large scale winds con-
 264 ditions in the lower stratosphere are almost as during phase one at balloons altitudes (end
 265 of eastward QBO phase).

266 In the following we will compare the momentum fluxes derived from the balloon
 267 data, emphasize the intrinsic frequencies that the scheme represents (the intrinsic peri-
 268 ods below 1hr) and consider the ERA5 data at the points that are the nearest from
 269 the balloon. The prediction is then made every hour and averaged over the day, partly
 270 because it is the time scale needed for the some schemes to sample realistically a GW
 271 field, and also because it takes around a day for a balloon flight to cover a model grid-
 272 scale. Note that some of the sensitivities to these choices are discussed in the Lott et al.
 273 (2023)’s conclusion.

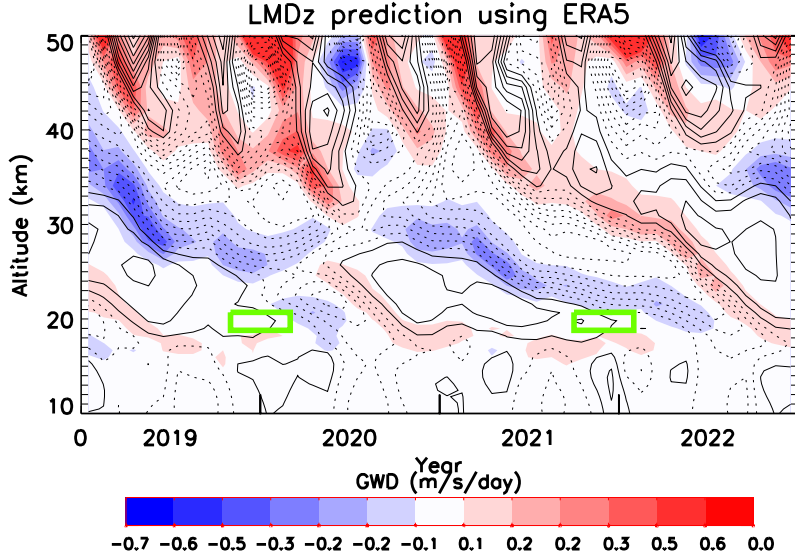


Figure 2. Time vertical sections of the zonal mean zonal wind (CI=10m/s, negative values are dashed and non-orographic gravity wave tendency averaged over the Equatorial band ($-6^{\circ}S - +6^{\circ}N$). Input data are from ERA5 reanalysis and GWs prediction from the LMDz scheme. The 2 green boxes indicate schematically the altitude and time ranges of the Strateole 2 phase 1 and 2 flights considered in this study.

3 Results

274

275 Figure 3 shows time series of daily values of momentum fluxes predicted by the pa-
 276 rameterizations and measured during balloon flights 2 from strateole 2 phase 1. This is
 277 also the flight shown in Fig. 3 in Lott et al. (2023), and where was also shown the time
 278 series of daily precipitation and zonal wind at flight altitude. The top panel is for the
 279 WMI based schemes, the middle panel for the HDS schemes and the bottom panels for
 280 the schemes relating the GWs fluxes to their sources. In all panels the black curves are
 281 for the daily observations. For clarity we present results for the Eastward and westward
 282 MFs only. Overall ones sees that the schemes predict momentum flux values that some-
 283 how compare with the observed one, at least in term of amplitude. There are neverthe-
 284 less significant differences in behaviour. For instance, the IFS's schemes present substan-
 285 tial peaks in eastward flux during the second half of the flight, which is a period during
 286 which the zonal wind at flight altitude becomes westward (see Figure 3b in Lott et al.
 287 (2023)), potentially favoring eastward waves, a process we refer to as dynamical filter-
 288 ing in (Lott et al., 2023) (see Eq. 3 there and the following discussion). Note that in this
 289 paper, we showed that the 3 peaks in measured fluxes around days 60, 75, and 83 also
 290 correspond to dates when there are precipitations near the balloon location. These cor-
 291 respondences made us believe that the relation with convective sources is essential, we
 292 see here that dynamical filtering alone may well be the main cause. Although having smaller
 293 amplitudes, the Figure show that in EC-Earth, the momentum fluxes behave almost as
 294 in IFS. The results from CMAM are quite different nevertheless. In this model it was
 295 chosen to place the launching altitude near the tropopause the daily series present much
 296 less fluctuations and long lasting "plateaus", clearly in this model, the distance between
 297 the launching level (100hPa see Table 2.1) and the balloon altitude is too small for dy-
 298 namical filtering to be efficient. The second panel for the HDS schemes is not fundamen-
 299 tally different from what was discussed above. The amplitude and fluctuations are com-
 300 parable to observed, some schemes predicting values which look either larger or smaller

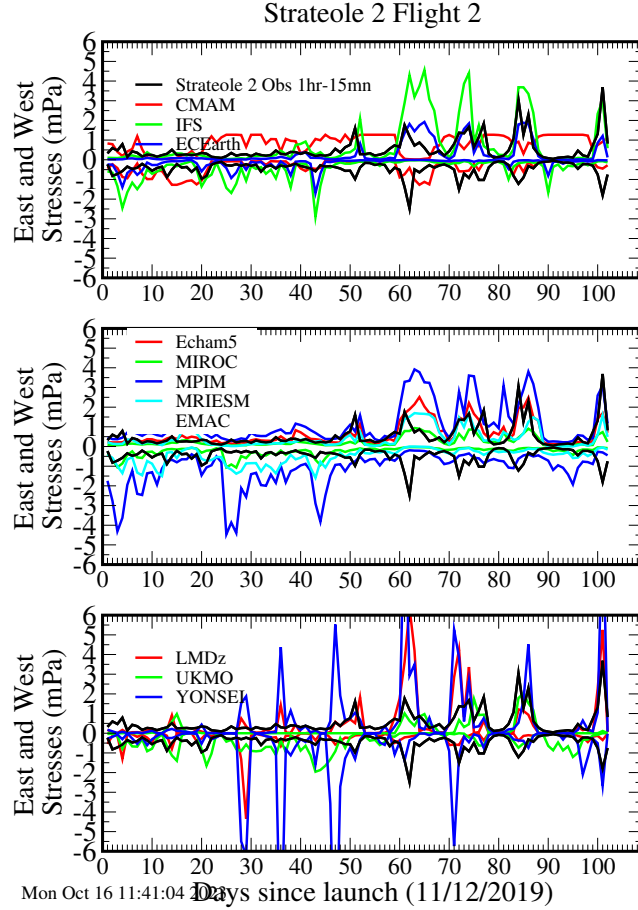


Figure 3. Comparison between daily averaged values of the eastward and westward MFs measured by the balloons during Strateole 2 phase 1 Flight 2 and estimated by the GW schemes at the balloon location and altitude. Colored curves are for the GW schemes predictions using ERA5 and from different models, black curves are for the observed MFs due to the 15mn-1hr GWs. a) WMI schemes; b) HDS Schemes; c) Multiwaves schemes relating launched MFs with convective sources or precipitations.

301 but staying within the range of observations. The behaviour of the source related schemes
 302 in the last panel is more contrasted. As expected, there are long periods during which
 303 the schemes predicted small and null momentum fluxes, interrupted by short last-
 304 ing peaks with values easily going beyond $\pm 5\text{mPa}$, values that were never reached by any
 305 of other schemes during this flight. In contrast with LMDz and YONSEI, the UKMO
 306 scheme present smaller amplitude and broader peaks, we attribute this to that it relates
 307 the launched flux to $\sqrt{P_r}$ rather than P_r^2 in LMDz, or the square of heating in YON-
 308 SEI's.

309 An other example of timeseries is provided in Fig. 4, which corresponds to a flight
 310 during the second phase of strateole 2. Beyond the fact that the flight is shorter than
 311 in Fig. 3, a difference in duration that characterize most of the flights during phase 2, the
 312 overall behaviours stay about the same, with the spectral schemes presenting fluctua-
 313 tions with broader peaks, except maybe CMAM, again because the launching altitude
 314 is quite high and dynamical filtering not yet efficient at balloon flight altitude. The last
 315 panel also shows that UKMO present long periods with almost no fluxes, in it, the fact

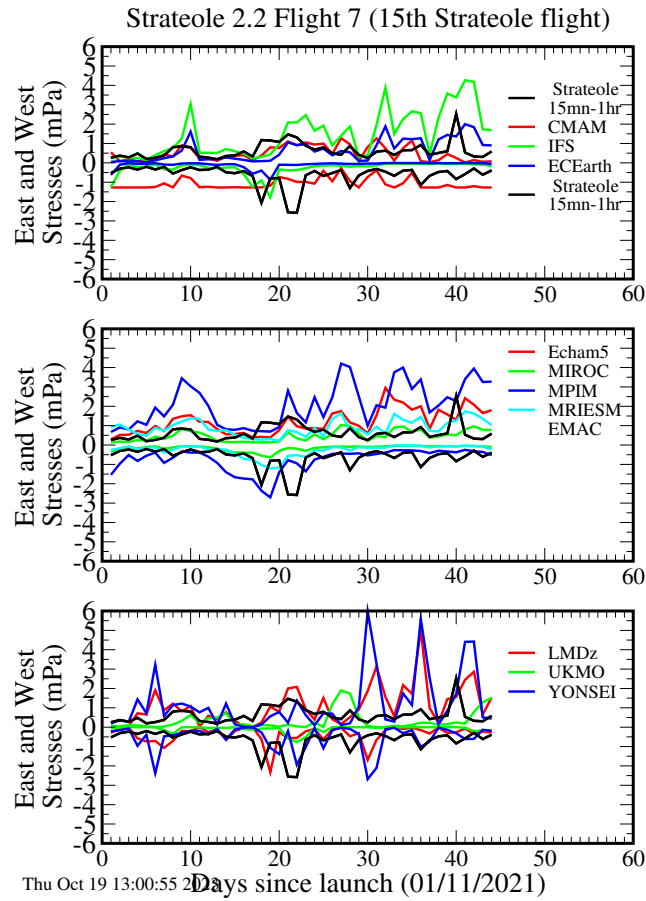


Figure 4. a) Same as Fig 2 but for Strateole 2 Phase 2 Flight 7.

316 that the launching height is near the surface produces much more critical level situations
 317 during the propagation through the tropopause.

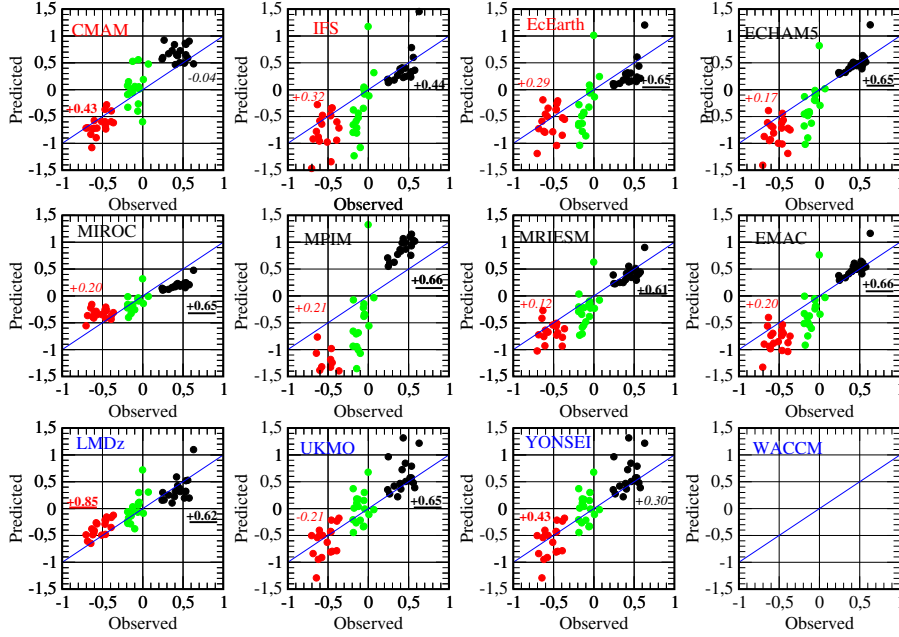


Figure 5. Scatter plot of the momentum fluxes measured by the balloon versus parameterized using different models. Only considered here the 18 balloon flights that last more than a month (East: black; West: red; Cumulated: green). Also shown are the correlations between observations and predictions, 99% significant levels are bold underlined, 95% are bold. Non significant values are shown in italic for information. The number of DoF for Pearson test is 18, about the number of balloon flights that last more than a month.

318 The fact that the different schemes estimate momentum fluxes of about the right
 319 amplitude is summarized in Fig. 5 where the average of the fluxes over the 18 flights that
 320 last more than a month (8 during phase 1, 10 during phase 2) are shown. In it we see
 321 that the predicted values align quite well with the observed one, some schemes having
 322 tendency to slightly underestimate the fluxes (MIROC, LMDz), other to overestimate
 323 them (CMAM, YONSEI), with the tendency to overestimate being in general more pro-
 324 nounced for the westward fluxes. The numbers in each panels also show the correlation
 325 between the 18 values averaged over each flights, showing that the correlations become
 326 strong in many models, at least in the eastward direction. Interestingly some models also
 327 have significant medium to high correlations in the westward direction (CMAM, LMDz,
 328 YONSEI).

329 The Figure 6 group the models averaging the eastward and westward fluxes over
 330 all the balloon flights, confirming again that the parameterizations used fall around the
 331 observed values. There is variabilities between the models, but there is no systematic
 332 tendency among the modellers to overstate or understate the MF's flux amplitude. This
 333 is summarized by the green curve which represents the average over models and over bal-
 334 loon flights. The average amplitude of the eastward flux is very near that observed (a
 335 10% overestimation between 0.45mPa in parameterizations against 0.40mPa observed),
 336 whereas the westward flux are overestimated by the models by less than 20% (-0.65mPa
 337 parameterized against -0.55mPa observed). This 10%-20% errors explain the quite large

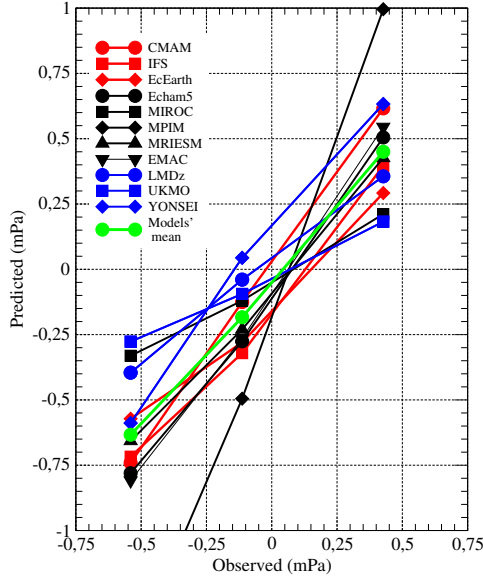


Figure 6. East, West and cumulated zonal momentum fluxes averaged over the Strateole 2 phase 1 and 2 period and according to participating models.

338 relative error (50%) in the cumulated flux but for it the large relative error is in good
 339 due to the fact that large positive and negative fluxes opposed each other.

340 The daily series in Figs 3 and 4 also suggest that observations and offline estima-
 341 tions sometimes evolve similarly day after day, a reason could be that both measured
 342 and parameterized MFs are sensitive to dynamical filtering, some schemes also taking
 343 into account sources. In the two examples given here, it is quite apparent in the first (Fig-
 344 ure 3) and for instance for the peaks in the eastward direction as already discussed. Cor-
 345 respondences are less obvious to visualize in the second case (Figure 4) where the evo-
 346 lution of the measured MFs present less variations than the predicted MFs. In (Lott et
 347 al., 2023) we analysed these daily variabilities flights by flights and indeed found that
 348 is some flights the series correlate well whereas in others they do not. The contrast be-
 349 tween flights made that in the end the correlations were significant but "medium" in
 350 the eastward direction $C \approx 0.5$ and "low" in the westward direction $C \approx 0.3$. Here
 351 and the following, we referred to "medium" positive correlations with $0.3 < C < 0.5$
 352 and small correlations when $0.1 < C < 0.3$. As such a result was obtained from the LMDz
 353 parameterization during Strateole 2 phase 1 the coefficients are given again in the 9th
 354 column of Table 4. In it are also given the same coefficients but for Phase 2, confirm-
 355 ing with an independent datasets the results in Lott et al. (2023). Consistent with Lott
 356 et al. (2023) but evaluating correlations over phases 1 and 2, we indeed found medium
 357 correlation in the Eastward phase ($C = 0.4$) and small in the westward phase ($C =$
 358 0.34). Here and for completeness, note that as in (Lott et al., 2023), and to test the sig-
 359 nificance, we measure the number of Degrees of Freedom (DoF) present in each dataset,
 360 and calculate for that the decorrelation time scale, which we take as the lag in day be-
 361 yond which the lag-autocorrelation of the series falls below 0.2. As this time-lag varies
 362 from one series to the other, we give explicitly in column 5, the number of DoF, which
 363 is the duration of the flight divided by the decorrelation time scale. Note that for their
 364 decorrelation time, we consider for simplicity that evaluated with daily averaged obser-
 365 vations, but found that it is not much different from that evaluated with the offline esti-
 366 mates (not shown).

East	Day Dof	CM AM	IFS	ECE ARTH	Ech am5	MI ROC	MPI M	MRI ESM	EM AC	LMD z	UK MO	YON SEI
Phase 1	670-216	-0.07	0.53	0.52	0.52	0.48	0.49	0.44	0.48	0.51	0.34	0.32
Phase 2	621-322	-0.19	0.41	0.38	0.38	0.33	0.34	0.30	0.33	0.40	0.34	0.20
Phase 1+2	1291-538	-0.11	0.49	0.47	0.45	0.41	0.41	0.36	0.40	0.46	0.34	0.27
West	Day Dof	CM AM	IFS	ECE ARTH	Ech am5	MI ROC	MPI M	MRI ESM	EM AC	LMD z	UK MO	YON SEI
Phase 1	670-216	0.14	-0.07	-0.07	-0.13	-0.03	-0.04	-0.04	-0.04	0.29	-0.03	0.10
Phase 2	621-322	0.21	0.18	0.16	0.03	0.00	0.01	0.05	-0.01	0.40	0.04	0.13
Phase 1+2	1291-538	0.17	0.05	0.04	-0.05	-0.02	-0.02	0.01	-0.02	0.34	0.00	0.11

Table 4. Correlation between observed and measured fluxes, stratoole phases 1 and 2.

367 If we now look at the schemes used in the other models, the result are contrasted
368 but quite in agreement. A lot a variations between flights (not shown) the overall be-
369 haviour being well summarized in the global correlation coefficients shown in Table 4.
370 First, and as for LMDz, the correlations evaluated using Phase 2 data stay robust when
371 compared to correlations evaluated using phase 1, and whatever is the level of correla-
372 tion ("medium", "low", or "non significant"). Second, is that many schemes managed
373 to have "medium" correlations ($0.3 < C < 0.5$) in the eastward direction, except the
374 CMAM scheme. We attribute this to the fact that in this model the launching level is
375 near the tropopause which strongly mitigates dynamical filtering. Also interesting, the
376 YONSEI scheme is the one is the lowest correlation after CMAM, in case of deep con-
377 vections it also launch waves from quite high levels in the troposphere suggesting that
378 in it as well and for some waves with strong eastward flux, dynamical filtering did not
379 have time to differentiate the waves between the launching level and the balloon level.
380 The results in the westward direction are more intriguing, the correlations are always
381 small except for 1 scheme (LMDz) and some but "low" correlations are found for the two
382 schemes that launch waves quite near the tropopause. We have difficulties in interpret-
383 ing this last result, it may be tells that the approaches where some waves are launched
384 from near the tropopause should not be disregarded, and that launching from a fixed al-
385 titude well in the tropospheres fails in some cases. But if this is the case, the performance
386 of LMDz are somehow in contradiction, in it the launching level is in the mid troposphere,
387 as many other schemes according to tables 2.1-2.1-2.1, maybe its skill come from the fact
388 that LMDz explicitey launch waves according to their intrinsic frequency at launch level
389 a property that is maybe more indirect in the spectral schemes.

390 **Controversy here? Are we right when writting the above two lines? They are quite**
391 **vague and can be deleted.**

392 Whatever is the explanation, it is maybe more interesting to notice that there is
393 room to improve GWs parameterizations to obtain better fits between predicted and mea-
394 sured fluxes in both directions of propagation.

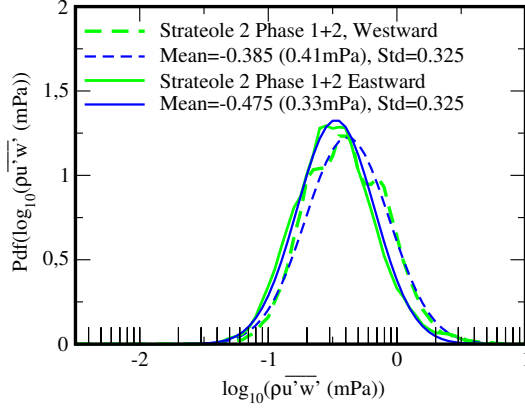


Figure 7. PDFs of daily values of Momentum flux distribution evaluated from Strateole Phases 1 and 2. The PDFs are calculated from histograms of 1291 MFs daily value within intervals of $\Delta(\log_{10} \rho \overline{u'w'}(\text{mPa})) = 0.05$, thereafter smoothed by a 5 point non-recursive filter with weight (0.1, 0.2, 0.4, 0.2, 0.1). Measured values are in green, log normal fits are in blue. Solid lines are for Eastward, dashed lines are for Westward. Here the log normal probability density function is defined as $P(X) = \frac{1}{\sqrt{2\pi}\sigma} e^{-\frac{(X-M)^2}{2S^2}}$, where $X = \log_{10} \rho |u'w'|$, and M and S the mean and standard deviations given in caption.

395 As said in the introduction, more than predicting the right fluxes at the right time,
 396 it is often believed that parameterizations should better be validated against their global
 397 statistical behaviour. A reason is that observed gravity waves show a strong level of in-
 398 termittency such an intermittency impacting the the effect of the waves on the large scale
 399 flow and climate in the middle atmosphere. In a recent Paper, Green et al. (2023) showed
 400 that this behaviour is well captured when the GWs MFs have pdfs following a log-normal
 401 distribution. These authors even concluded that in all directions of propagation, momen-
 402 tum fluxes characteristics could be summarized in terms terms of the mean and variance
 403 of log normal distributions. As shown before in (Lott et al., 2023) such lognormal dis-
 404 tributions describe well the Strateole-2 data, a behaviour illustrated further well when
 405 evaluating the pdfs over phase 1 and 2 (see Fig. 7. One also sees that the balloons al-
 406 most systematically measure fluxes with amplitude between 0.1mPa and 10mPa, the pdf
 407 of the westward fluxes being shifted toward higher values compared to that for eastward
 408 flues the shapes being little changed.

409 To analyse our schemes in this framework the Figure 8 presents PDFs of the dis-
 410 tributions of the momentum fluxes considering all the daily data. For the observed PDFs
 411 (green solid for eastward fluxes, green dashed for westward fluxes), When one consider
 412 the parameterizations schemes, one notice that the pdf are often much broader than the
 413 observed pdfs with the WMI schemes than whereas the HDS schemes seem more real-
 414 istic in this respect. The HDS schemes are also those for which the shift of the westward
 415 pdf toward higher values is the more realistically reproduced. Finally, the schemes that
 416 relate GWs to convection systematically have much broader pdfs, they all present a tail
 417 toward small values of the MFs, suggesting that in them miss a background of wave ac-
 418 tivity existing even in the absence of convection nearby.

419 We also notice that the in all models, the pdf of the westward fluxes are shifted to
 420 higher values compared to the pdfs of the eastward fluxes, and this is consistent with the
 421 fact that in an easterly phase, waves in the westward direction can reach larger ampli-
 422 tudes than the waves in the eastward direction (dynamical filtering again and always con-
 423 sistent with observations). To a large extent, and for most of the spectral scheme this

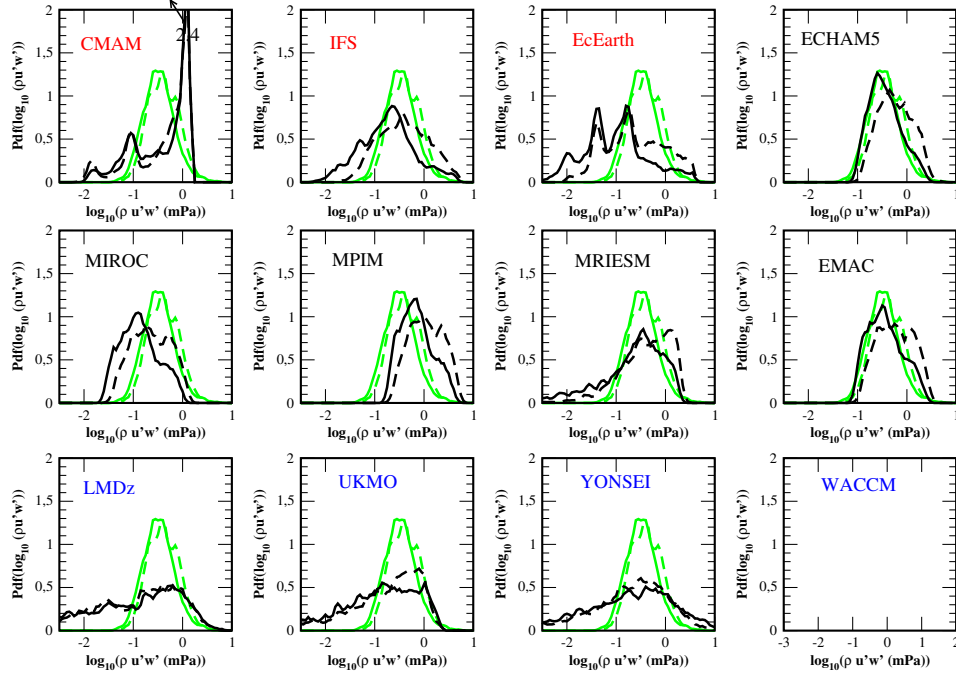


Figure 8. PDFs of daily values of Momentum flux distribution, same method as in Fig. 7. Measure values are in green, estimations using ERA5 data and the parameterizations are in black. Solid lines are for Eastward, dashed lines are for Westward.

424 supports the results in Green et al. (2023) where the difference in GW momentum fluxes
 425 between direction of propagations could essentially be summarized by log-normal pdfs
 426 shifted by differences in mean values.

427 4 Conclusion

428 The main result of this paper is that state of the art parameterizations of GWs re-
 429 produce reasonably well the momentum flux due to the high-frequency waves (periods
 430 between 15mn and 1hr) deduced from in situ measurements made onboard constant-level
 431 balloons. The parameterizations represent well the eastward and westward values of the
 432 stress and in some cases their variations from day to day. Although the various schemes
 433 performed differently regarding the day to day correlations, our results show that im-
 434 provement can be done in this regard. Some scheme for instance present "medium" cor-
 435 relations in the eastward direction, telling that such correlation levels can be reached.
 436 In the westward direction, the day to day correlations are "low", to the best and in 1
 437 model, we can only say that such a level can also be reached in the tropical regions.

438 Due to the low to medium level of correlations we found, we could ask ourselves
 439 if it is mandatory to improve GW schemes according to such a criteria. After all, when
 440 the momentum fluxes are averaged over periods near a month (here we rather consider
 441 averages over balloon flights), the correlations become "medium" to "strong" in the east-
 442 ward direction (see 5) and frequently medium in the westward direction, which is prob-
 443 ably enough in the context of the QBO forcing, the QBO evolving over time scales much
 444 larger than a month.

445 An other substantial difference concerns the pdfs of the parameterized momentum
 446 fluxes against those of the measured fluxes. Many spectral schemes have log-normal pdfs

447 consistent with observations, providing that the launch level is not too close from the bal-
448 loon location, whereas the schemes that relate the GWs to their convective sources all
449 present tails toward small values which seem unrealistic. As intermittency is a key fac-
450 tor controlling the altitude at which GWs break, a factor that can have climatic impacts
451 ((de la Cámara et al., 2016)), this should be considered seriously, at least by introduc-
452 ing a background in wave launching amplitude in the schemes that only consider con-
453 vective sources. This issue may well also be partly sorted out by introducing lateral prop-
454 agation (Amemiya & Sato, 2016), a process that is important in the balloon observations
455 used here (Corcos et al., 2021), but this will not be sufficient over quite large and dry
456 regions.

457 We did not try to fit the parameters of the schemes we use in order to improve daily
458 correlations or pdfs or both, but we plan to do it in the near future. We have not much
459 data though, but could use the Loon data post-processed in a comparable way as Stra-
460 teole 2 by (Green et al., 2023), which would permit to cover much wider regions. We should
461 also test if improving the schemes parameters to improve the fit with observations im-
462 prove or do not degrade the models climate. It well may be that parameterizations com-
463 pensate for potentially resolved equatorial waves for instance, the latter showing a lot
464 of variability between the QBOi models (Holt et al., 2022). Also, we could also hope that
465 a better fit with observed values would help reduced persistent systematic errors in the
466 QBO simulations, one of them being that models underestimate the QBO amplitude in
467 the low stratosphere. Unfortunately, our results so far are not much positive: a common
468 believe is that such an error could well be reduced by launching waves from near the tropopause,
469 the only model which do so here is not much realistic when it comes to predict MFs vari-
470 abilities.

5 Open Research

Balloon data presented in Haase et al. (2018) can be extracted from the STRATEOLE 2 dedicated web site: <https://webstr2.ipsl.polytechnique.fr>

ERA5 reanalysis data are described in Hersbach et al. (2020) and can be extracted from the COPERNICUS access hub: <https://scihub.copernicus.eu/>

The LMDz-6A GCM used for CMIP6 project is described in Hourdin et al. (2020), it can be directly installed from the dedicated webpage: <https://lmdz.lmd.jussieu.fr/utilisateurs/installation-lmdz>

Acknowledgments

This work was supported by the VESRI Schmidt Future project "DataWave".

Appendix: Running the offline code

To run the models parameterizations in offline mode and compare with daily values of momentum fluxes measured during strateole 2, download the file `offline_v9_Strateole_QBOi_Open.tar`, on the web page:

```
wget https://web.lmd.jussieu.fr/~flott/DATA/offline_v9_Strateole_QBOi_Open.tar.gz
```

Then gunzip and do `tar -xvf offline_v9_Strateole_QBOi_Open.tar`

In the directory, `offline_v9_Strateole_QBOi_Open`:

Run directory It basically contains a script that compile the programs, link to the input dataset and produce various outputs. The Makefile certainly needs to be adapted to the computer.

To launch predictions for Strateole-2 phase 1, launch: `./laun_ph1ball_gwd_era5.sh`
For phase 2, `ph1` → `ph2`.

Fortran Codes: all the fortran routines are located in `prog`.

laun_gwd_era5.f90: Main program loading input data in netcdf format and calculating drag and momentum fluxes at the balloon place.

preci_gwd_LMDz_QBOi.f90: LMDz Multiwaves routines predicting gwdrag from precipitation

gwsat_Modnam.f90: the globally spectral scheme using the Warner and McIntyre (1996)'s scheme version by J. Scinocca.

hinesgw6g_plus_subs.f HDS scheme

gw_ussp_core.f90: The WMI scheme with amplitude keyed to precipitation used in some UKMO runs.

cgwcalc.f90: Multiwave scheme developped at Yonsei's university

Input Data: All the input data are located in the directories `hourly_ph1` and `hourly_ph2` for phase 1 and 2 respectively. For instance, 1hr average of the strateole2 momentum fluxes are in

`ALL_STRATEOLE2_Balloon_ph1_1day15min.nc`
and

`ALL_STRATEOLE2_Balloon_ph1_1hrs15min.nc`

for the waves with periods between 1day and 15mn and between 1Hr and 15 mn respectively.

Still in this directory, the ERA5 reanalysis products, which include winds temperature, cloud liquid water, and surface log pressure, over a $5^\circ \times 5^\circ$ domain centered at the balloons drifting locations are in `Input_ERA5_data_all_variables_balloons_ph1.nc`. Precipitation every hours are also included. The diabatic heatings are from fore-

517 cast. All datas that are only provided every 3hr are linearly interpolated in time
 518 to give hourly values.

519 Output data (Part 1)

520 All the outputs are in the output_ph1 and output_ph2 directories:

521 **Netcdf:** contains the output of the schemes in netcdf format on the vertical col-
 522 umn and over the 5°x5° domain over which the ER5 data are provided. There is
 523 one netcdf dataset by balloons flight each contains output from all the schemes.

524 **Balloon_alt** After post processing by the python scripts launch_script_obs.py, are
 525 extracted the MFs at balloon flight altitude.

526 Python Scripts

527 A serie of Python scripts, located into python_script are proposed to compare the
 528 outputs of the scheme to the balloon data.

529 **launch_script_obs.py:** Reads the balloon flight data of MFs and averaged over
 530 1day and writte them in text format (ending with '.dat') and stored in **output/Balloon_alt/obs_output**

531 **launch_prediction_eachB_ysei.py:** extract from the prediction the values of the
 532 MFs at the balloons place and altitude. Results stored in text format (".dat" in
 533 **Balloon_alt/Pred_output_Balloon_altitude/**.

534 The next python scripts are cosmetic in the sense that they use the above two datasets
 535 to make plots of timeseries balloon averaged values, evaluate correlations, and his-
 536 tograms.

537 **timeseries_obs_pred_plot_all.py** Produces a lot of time series for each model
 538 and flights.

539 Output data (Part2) As a result, you can visualize timeseries of each flight here:

540 **output_ph1/Balloon_alt/figure_timeseries**

541 Histograms here: **output_ph1/histo**

542 Scatter plots and correlations here **output_ph1/correlation**

543 For phase 2, change ph1 in ph2.

544 xmgrace Alternative to calculate these diagnostics using fortran programs and xmgrace,
 545 the programs permit to combine statistics over the 2 phases of Strateole2.

546

References

547

Alexander, M. J., Beres, J. H., & Pfister, L. (2000). Tropical stratospheric gravity wave activity and relationships to clouds. *Journal of Geophysical Research: Atmospheres*, *105*(D17), 22299–22309. doi: <https://doi.org/10.1029/2000JD900326>

551

Alexander, M. J., & Dunkerton, T. J. (1999). A Spectral Parameterization of Mean-Flow Forcing due to Breaking Gravity Waves. *J. Atmos. Sci.*, *56*(24), 4167–4182. doi: 10.1175/1520-0469(1999)056<4167:ASPOMF>2.0.CO;2

553

554

Alexander, M. J., Geller, M., McLandress, C., Polavarapu, S., Preusse, P., Sassi, F., . . . Watanabe, S. (2010). Recent developments in gravity-wave effects in climate models and the global distribution of gravity-wave momentum flux from observations and models. *Q. J. R. Meteorol. Soc.*, *136*, 1103–1124. doi: <https://doi.org/10.1002/qj.637>

558

559

Alexander, M. J., Liu, C. C., Bacmeister, J., Bramberger, M., Hertzog, A., & Richter, J. H. (2021). Observational validation of parameterized gravity waves from tropical convection in the whole atmosphere community climate model. *Journal of Geophysical Research: Atmospheres*, *126*(7), e2020JD033954. (e2020JD033954 2020JD033954) doi: <https://doi.org/10.1029/2020JD033954>

562

563

Amemiya, A., & Sato, K. (2016). A new gravity wave parameterization including three-dimensional propagation. *Journal of the Meteorological Society of Japan. Ser. II*, *94*(3), 237–256. doi: 10.2151/jmsj.2016-013

566

567

Andrews, F. G., Holton, J., & Leovy, C. (1987). *Middle atmosphere dynamics*. Academic Press.

568

569

Anstey, J. A., Scinocca, J. F., & Keller, M. (2016). Simulating the qbo in an atmospheric general circulation model: Sensitivity to resolved and parameterized forcing. *Journal of the Atmospheric Sciences*, *73*(4), 1649 - 1665. doi: <https://doi.org/10.1175/JAS-D-15-0099.1>

571

572

Baldwin, M. P., Gray, L. J., Dunkerton, T. J., Hamilton, K., Haynes, P. H., Randel, W. J., . . . Takahashi, M. (2001). The quasi-biennial oscillation. *Rev. Geophys.*, *39*(2), 179–229. doi: 10.1029/1999RG000007

573

574

Beres, J. H., Garcia, R. R., Boville, B. A., & Sassi, F. (2005). Implementation of a gravity wave source spectrum parameterization dependent on the properties of convection in the whole atmosphere community climate model (waccm). *Journal of Geophysical Research: Atmospheres*, *110*(D10). doi: <https://doi.org/10.1029/2004JD005504>

576

577

Bushell, A. C., Butchart, N., Derbyshire, S. H., Jackson, D. R., Shutts, G. J., Vosper, S. B., & Webster, S. (2015). Parameterized gravity wave momentum fluxes from sources related to convection and large-scale precipitation processes in a global atmosphere model. *Journal of the Atmospheric Sciences*, *72*(11), 4349–4371. doi: <https://doi.org/10.1175/JAS-D-15-0022.1>

583

584

Butchart, N., Anstey, J. A., Hamilton, K., Osprey, S., McLandress, C., Bushell, A. C., . . . Yukimoto, S. (2018). Overview of experiment design and comparison of models participating in phase 1 of the sparc quasi-biennial oscillation initiative (“qboi”). *Geoscientific Model Development*, *11*(3), 1009–1032. doi: 10.5194/gmd-11-1009-2018

586

587

Charron, M., & Manzini, E. (2002). Gravity waves from fronts: Parameterization and middle atmosphere response in a general circulation model. *Journal of the Atmospheric Sciences*, *59*(5), 923 - 941. doi: 10.1175/1520-0469(2002)059<0923:GWFFPA>2.0.CO;2

591

592

Choi, H.-J., & Chun, H.-Y. (2011). Momentum flux spectrum of convective gravity waves. part i: An update of a parameterization using mesoscale simulations. *Journal of the Atmospheric Sciences*, *68*(4), 739 - 759. doi: <https://doi.org/10.1175/2010JAS3552.1>

595

596

Christiansen, B., Yang, S., & Madsen, M. S. (2016). Do strong warm enso events control the phase of the stratospheric qbo? *Geophysical Research Letters*,

599

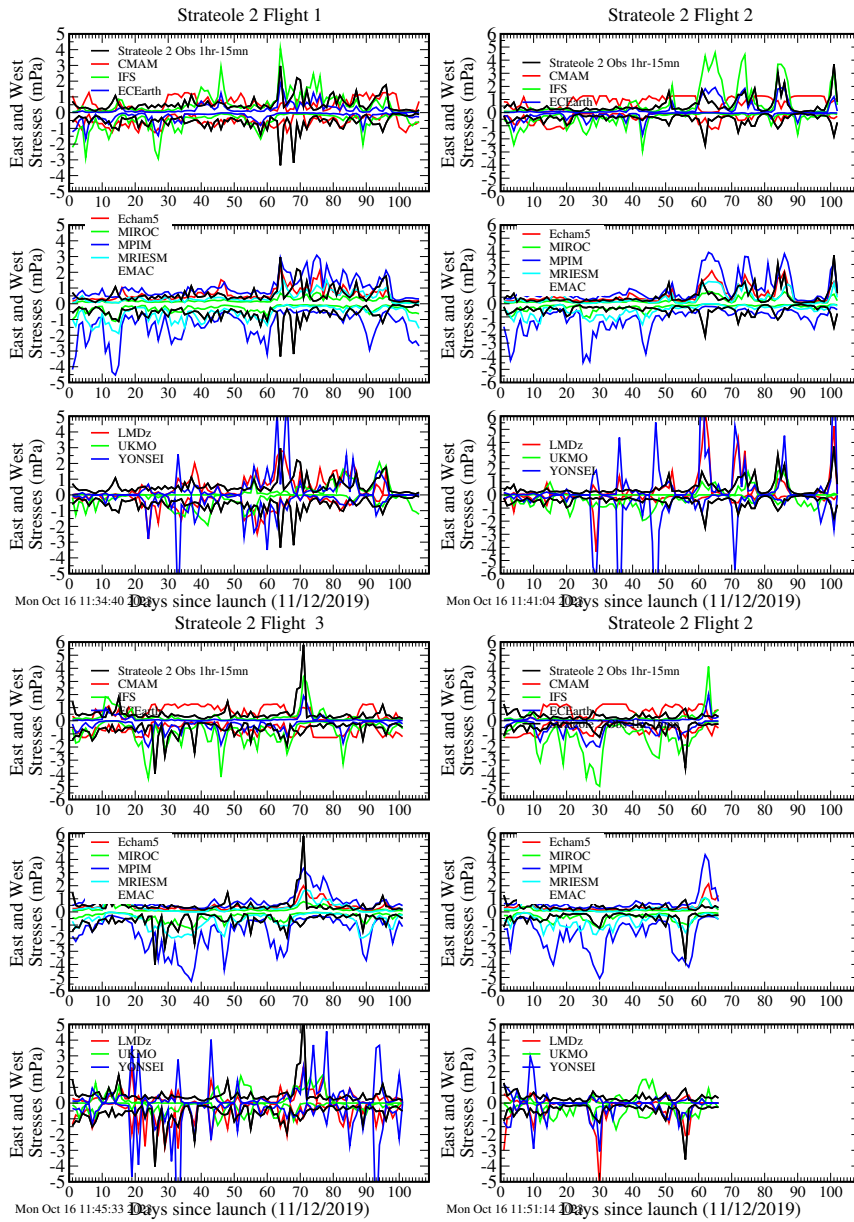
600

- 601 43(19), 10,489-10,495. doi: <https://doi.org/10.1002/2016GL070751>
- 602 Corcos, M., Hertzog, A., Plougonven, R., & Podglajen, A. (2021). Observation of
603 gravity waves at the tropical tropopause using superpressure balloons. *Journal*
604 *of Geophysical Research: Atmospheres*, 126(15), e2021JD035165. doi: [https://](https://doi.org/10.1029/2021JD035165)
605 doi.org/10.1029/2021JD035165
- 606 Davini, P., von Hardenberg, J., Corti, S., Christensen, H. M., Juricke, S., Subrama-
607 nian, A., ... Palmer, T. N. (2017). Climate sphinx: evaluating the impact
608 of resolution and stochastic physics parameterisations in the ec-earth global
609 climate model. *Geoscientific Model Development*, 10(3), 1383–1402. Re-
610 trieved from <https://gmd.copernicus.org/articles/10/1383/2017/> doi:
611 [10.5194/gmd-10-1383-2017](https://doi.org/10.5194/gmd-10-1383-2017)
- 612 de la Cámara, A., & Lott, F. (2015). A parameterization of gravity waves emit-
613 ted by fronts and jets. *Geophys. Res. Lett.*, 42(6), 2071-2078. doi: [10.1002/](https://doi.org/10.1002/2015GL063298)
614 [2015GL063298](https://doi.org/10.1002/2015GL063298)
- 615 de la Cámara, A., Lott, F., & Hertzog, A. (2014). Intermittency in a stochastic
616 parameterization of nonorographic gravity waves. *J. Geophys. Res.: Atmo-*
617 *spheres*, 119(21), 11905-11919. doi: [10.1002/2014JD022002](https://doi.org/10.1002/2014JD022002)
- 618 de la Cámara, A., Lott, F., Jewtoukoff, V., Plougonven, R., & Hertzog, A. (2016).
619 On the gravity wave forcing during the southern stratospheric final warming
620 in LMDZ. *J. Atmos. Sci.*, 73(8), 3213-3226. doi: [https://doi.org/10.1175/](https://doi.org/10.1175/JAS-D-15-0377.1)
621 [JAS-D-15-0377.1](https://doi.org/10.1175/JAS-D-15-0377.1)
- 622 Eckermann, S. D. (2011). Explicitly Stochastic Parameterization of Nonorographic
623 Gravity Wave Drag. *J. Atmos. Sci.*, 68, 1749–1765. doi: [10.1175/2011JAS3684](https://doi.org/10.1175/2011JAS3684.1)
624 [.1](https://doi.org/10.1175/2011JAS3684.1)
- 625 Ern, M., Ploeger, F., Preusse, P., Gille, J., Gray, L. J., Kalisch, S., ... Riese, M.
626 (2014). Interaction of gravity waves with the QBO: A satellite perspec-
627 tive. *Journal of Geophysical Research: Atmospheres*, 119, 2329 - 2355. doi:
628 <https://doi.org/10.1002/2013JD020731>
- 629 Fovell, R., Durran, D., & Holton, J. R. (1992). Numerical simulations of convec-
630 tively generated stratospheric gravity waves. *Journal of Atmospheric Sciences*,
631 49(16), 1427 - 1442. doi: [10.1175/1520-0469\(1992\)049<1427:NSOCGS>2.0.CO;](https://doi.org/10.1175/1520-0469(1992)049<1427:NSOCGS>2.0.CO;2)
632 [2](https://doi.org/10.1175/1520-0469(1992)049<1427:NSOCGS>2.0.CO;2)
- 633 Fueglistaler, S., Legras, B., Beljaars, A., Morcrette, J.-J., Simmons, A., Tomp-
634 kins, A. M., & Uppala, S. (2009). The diabatic heat budget of the up-
635 per troposphere and lower/mid stratosphere in ecmwf reanalyses. *Quar-*
636 *terly Journal of the Royal Meteorological Society*, 135(638), 21-37. doi:
637 <https://doi.org/10.1002/qj.361>
- 638 Geller, M. A., Alexander, M. J., Love, P. T., Bacmeister, J., Ern, M., Hertzog, A.,
639 ... Zhou, T. (2013). A comparison between gravity wave momentum fluxes in
640 observations and climate models. *J. Atmos. Sci.*, 26(17).
- 641 Green, B., Sheshadri, A., Alexander, M., Bramberger, M., & Lott, F. (2023). Grav-
642 ity wave momentum fluxes estimated from project loon balloon data. *Journal*
643 *of Geophysical Research: Atmospheres*, Submitted.
- 644 Haase, J. S., Alexander, M. J., Hertzog, A., Kalnajs, L. E., Deshler, T., Davis,
645 S. M., ... Venel, S. (2018). Around the world in 84 days [Dataset]. *Eos*, 99.
646 doi: <https://doi.org/10.1029/2018EO091907>
- 647 Hersbach, H., Bell, B., Berrisford, P., Hirahara, S., Horányi, A., Muñoz-Sabater,
648 J., ... Thépaut, J.-N. (2020). The ERA5 global reanalysis [Dataset]. *Quar-*
649 *terly Journal of the Royal Meteorological Society*, 146(730), 1999-2049. doi:
650 <https://doi.org/10.1002/qj.3803>
- 651 Hertzog, A. (2007). The stratéole-vorcore long-duration balloon experiment: A per-
652 sonal perspective. *Space Research Today*, 169, 43-48. Retrieved from [https://](https://www.sciencedirect.com/science/article/pii/S1752929807800478)
653 www.sciencedirect.com/science/article/pii/S1752929807800478 doi:
654 [https://doi.org/10.1016/S1752-9298\(07\)80047-8](https://doi.org/10.1016/S1752-9298(07)80047-8)
- 655 Hertzog, A., Alexander, M. J., & Plougonven, R. (2012). On the Intermittency

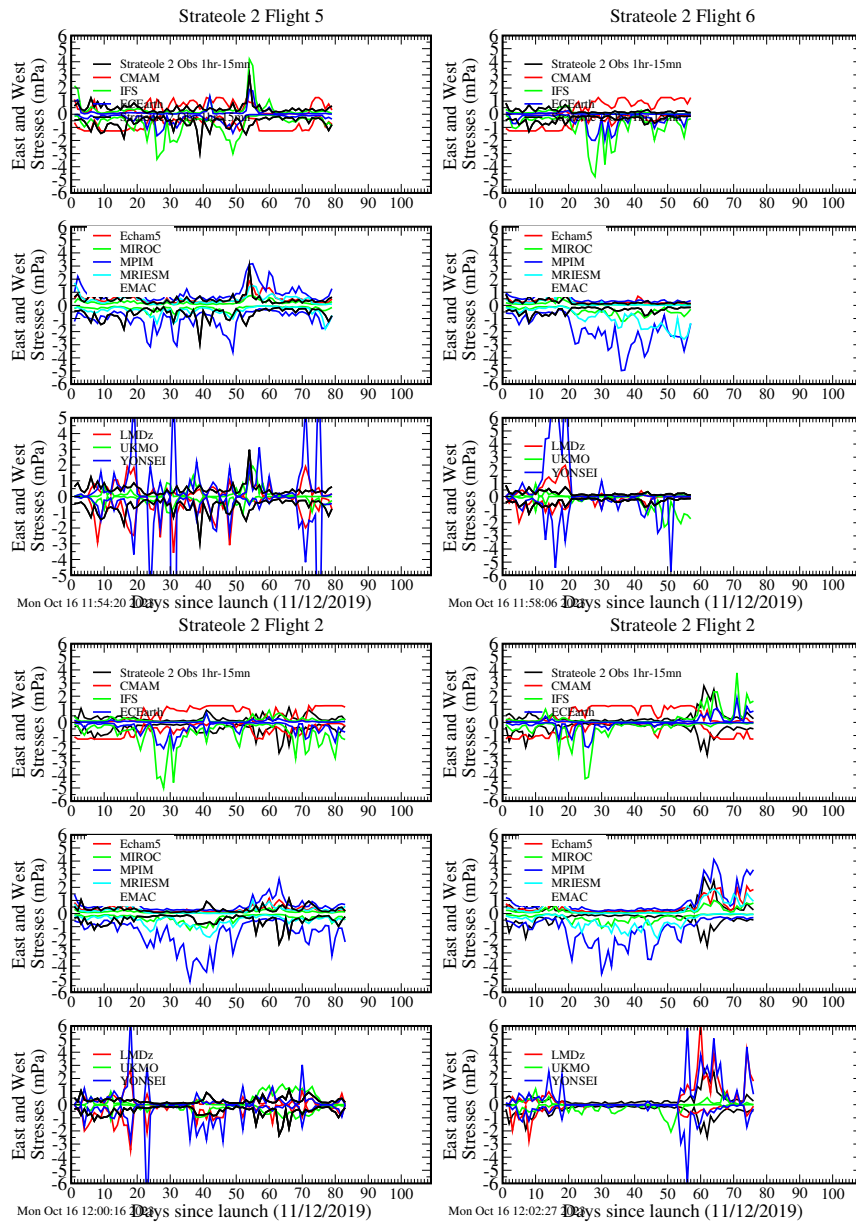
- of Gravity Wave Momentum Flux in the Stratosphere. *Journal of the Atmospheric Sciences*(11), 3433–3448. doi: 10.1175/JAS-D-12-09.1
- Hines, C. O. (1991). The saturation of gravity waves in the middle atmosphere. part ii: Development of doppler-spread theory. *Journal of Atmospheric Sciences*, 48(11), 1361 - 1379. doi: [https://doi.org/10.1175/1520-0469\(1991\)048<1361:TSGOWI>2.0.CO;2](https://doi.org/10.1175/1520-0469(1991)048<1361:TSGOWI>2.0.CO;2)
- Hines, C. O. (1997). Doppler-spread parameterization of gravity-wave momentum deposition in the middle atmosphere. part 2: Broad and quasi monochromatic spectra, and implementation. *J. Atmos. Solar Terr. Phys.*, 59(4), 387-400. doi: 10.1016/S1364-6826(96)00080-6
- Holt, L. A., Lott, F., Garcia, R. R., Kiladis, G. N., Cheng, Y.-M., Anstey, J. A., ... Yukimoto, S. (2022). An evaluation of tropical waves and wave forcing of the QBO in the QBOi models. *Quarterly Journal of the Royal Meteorological Society*, 148(744), 1541-1567. doi: <https://doi.org/10.1002/qj.3827>
- Hourdin, F., Rio, C., Grandpeix, J.-Y., Madeleine, J.-B., Cheruy, F., Rochetin, N., ... Ghattas, J. (2020). LMDZ6A: The atmospheric component of the ipsl climate model with improved and better tuned physics [Software]. *Journal of Advances in Modeling Earth Systems*, 12(7), e2019MS001892. doi: <https://doi.org/10.1029/2019MS001892>
- Jewtoukoff, V., Hertzog, A., Plougonven, R., de la Cámara, A., & Lott, F. (2015). Comparison of gravity waves in the southern hemisphere derived from balloon observations and the ecmwf analyses. *J. Atmos. Sci.*, 72(9). doi: DOI:10.1175/JAS-D-14-0324.1
- Jewtoukoff, V., Plougonven, R., & Hertzog, A. (2013). Gravity waves generated by deep tropical convection: Estimates from balloon observations and mesoscale simulations. *Journal of Geophysical Research: Atmospheres*, 118(17), 9690-9707. doi: <https://doi.org/10.1002/jgrd.50781>
- Kang, M.-J., Chun, H.-Y., & Kim, Y.-H. (2017). Momentum flux of convective gravity waves derived from an offline gravity wave parameterization. part i: Spatiotemporal variations at source level. *Journal of the Atmospheric Sciences*, 74(10), 3167 - 3189. doi: 10.1175/JAS-D-17-0053.1
- Lane, T. P., & Moncrieff, M. W. (2008). Stratospheric gravity waves generated by multiscale tropical convection. *J. Atmos. Sci.*, 65, 2598–2614. doi: DOI:10.1175/2007JAS2601.1
- Lindzen, R. S. (1981). Turbulence and stress owing to gravity wave and tidal breakdown. *J. Geophys. Res.*, 86(C10), 9707-9714. doi: 10.1029/JC086iC10p09707
- Liu, C., Alexander, J., Richter, J., & Bacmeister, J. (2022). Using trmm latent heat as a source to estimate convection induced gravity wave momentum flux in the lower stratosphere. *Journal of Geophysical Research: Atmospheres*, 127(1), e2021JD035785. (e2021JD035785 2021JD035785) doi: <https://doi.org/10.1029/2021JD035785>
- Lott, F., & Guez, L. (2013). A stochastic parameterization of the gravity waves due to convection and its impact on the equatorial stratosphere. *J. Geophys. Res.*, 118(16), 8897-8909. doi: 10.1002/jgrd.50705
- Lott, F., Guez, L., & Maury, P. (2012). A stochastic parameterization of non-orographic gravity waves: Formalism and impact on the equatorial stratosphere. *Geophys. Res. Lett.*, 39(6), L06807. doi: 10.1029/2012GL051001
- Lott, F., Rani, R., Podglajen, A., Codron, F., Guez, L., Hertzog, A., & Plougonven, R. (2023). Direct comparison between a non-orographic gravity wave drag scheme and constant level balloons. *Journal of Geophysical Research: Atmospheres*, 128(4), e2022JD037585. doi: <https://doi.org/10.1029/2022JD037585>
- Manzini, E., McFarlane, N. A., & McLandress, C. (1997). Impact of the doppler spread parameterization on the simulation of the middle atmosphere circulation using the ma/echam4 general circulation model. *Journal of Geophysical Research: Atmospheres*, 102(D22), 25751-25762. doi: 10.1029/97JD01096

- 711 Orr, A., Bechtold, P., Scinocca, J., Ern, M., & Janiskova, M. (2010). Improved mid-
712 dle atmosphere climate and forecasts in the ecmwf model through a nonoro-
713 graphic gravity wave drag parameterization. *Journal of Climate*, *23*(22), 5905
714 - 5926. doi: <https://doi.org/10.1175/2010JCLI3490.1>
- 715 Plougonven, R., Jewtoukoff, V., de la Cámara, A., Lott, F., & Hertzog, A. (2017).
716 On the relation between gravity waves and wind speed in the lower strato-
717 sphere over the southern ocean. *J. Atmos. Sci.*, *74*(4), 1075-1093. doi:
718 10.1175/JAS-D-16-0096.1
- 719 Rabier, F., Bouchard, A., Brun, E., Doerenbecher, A., Guedj, S., Guidard, V.,
720 ... Steinle, P. (2010, January). The Concordiasi Project in Antarctica.
721 *Bulletin of the American Meteorological Society*, *91*(1), 69-86. Retrieved
722 from <https://hal-insu.archives-ouvertes.fr/insu-00562459> doi:
723 10.1175/2009BAMS2764.1
- 724 Richter, J. H., Sassi, F., & Garcia, R. R. (2010). Toward a physically based gravity
725 wave source parameterization in a general circulation model. *Journal of the At-
726 mospheric Sciences*, *67*(1), 136 - 156. doi: 10.1175/2009JAS3112.1
- 727 Scaife, A. A., Butchart, N., Warner, C. D., & Swinbank, R. (2002). Impact of a
728 spectral gravity wave parameterization on the stratosphere in the met office
729 unified model. *Journal of the Atmospheric Sciences*, *59*(9), 1473 - 1489. doi:
730 [https://doi.org/10.1175/1520-0469\(2002\)059<1473:IOASGW>2.0.CO;2](https://doi.org/10.1175/1520-0469(2002)059<1473:IOASGW>2.0.CO;2)
- 731 Scinocca, J. F. (2003). An accurate spectral nonorographic gravity wave drag pa-
732 rameterization for general circulation models. *Journal of the Atmospheric Sci-
733 ences*, *60*(4), 667 - 682. doi: [https://doi.org/10.1175/1520-0469\(2003\)060<0667:
734 AASNGW>2.0.CO;2](https://doi.org/10.1175/1520-0469(2003)060<0667:AASNGW>2.0.CO;2)
- 735 Serva, F., Cagnazzo, C., Riccio, A., & Manzini, E. (2018). Impact of a stochastic
736 nonorographic gravity wave parameterization on the stratospheric dynamics of
737 a general circulation model. *Journal of Advances in Modeling Earth Systems*,
738 *10*(9), 2147-2162. doi: <https://doi.org/10.1029/2018MS001297>
- 739 Song, I.-S., & Chun, H.-Y. (2005). Momentum flux spectrum of convectively
740 forced internal gravity waves and its application to gravity wave drag pa-
741 rameterization. part i: Theory. *J. Atmos. Sci.*, *62*(1), 107-124. doi:
742 <https://doi.org/10.1175/JAS-3363.1>
- 743 Warner, C. D., & McIntyre, M. E. (1996). On the propagation and dissipation
744 of gravity wave spectra through a realistic middle atmosphere. *J. Atmos. Sci.*,
745 *53*(22), 3213-3235. doi: 10.1175/1520-0469(1996)053<3213:OTPADO>2.0.CO;
746 2
- 747 Warner, C. D., & McIntyre, M. E. (1999). Toward an ultra-simple spectral grav-
748 ity wave parameterization for general circulation models. *Earth, Planets and
749 Space*, *51*, 475-484. doi: 10.1186/BF03353209

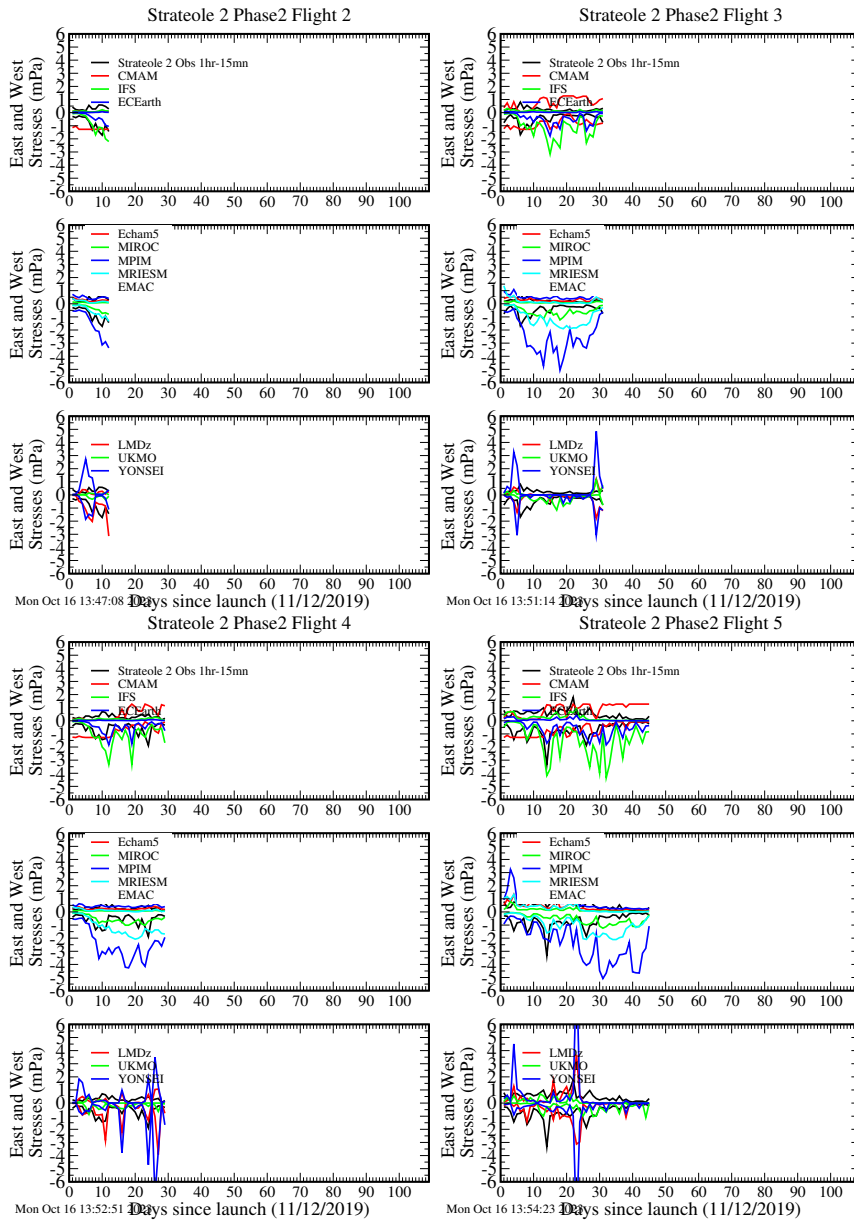
Supplementary: Phase 1 flights and models



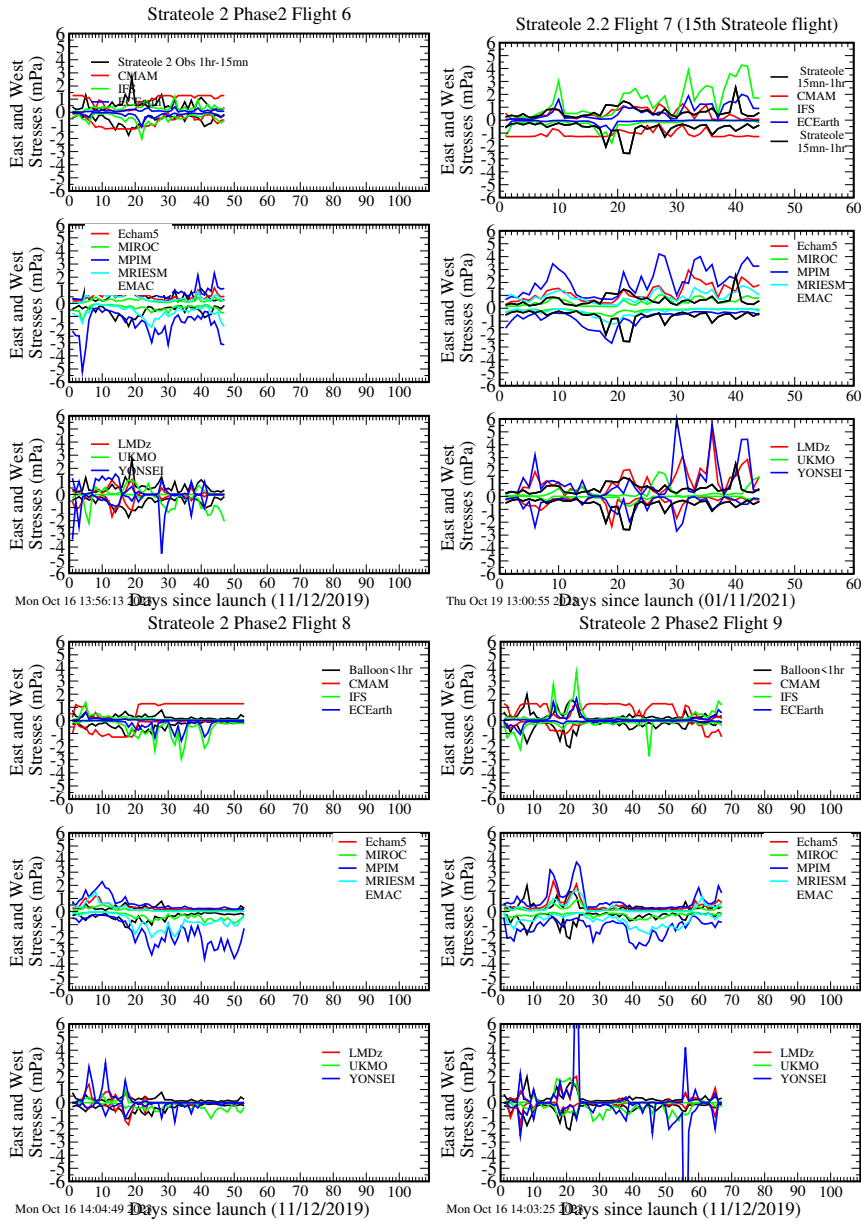
Supplementary: Phase 1 flights and models (continued)



Supplementary: Phase 2 flights and models

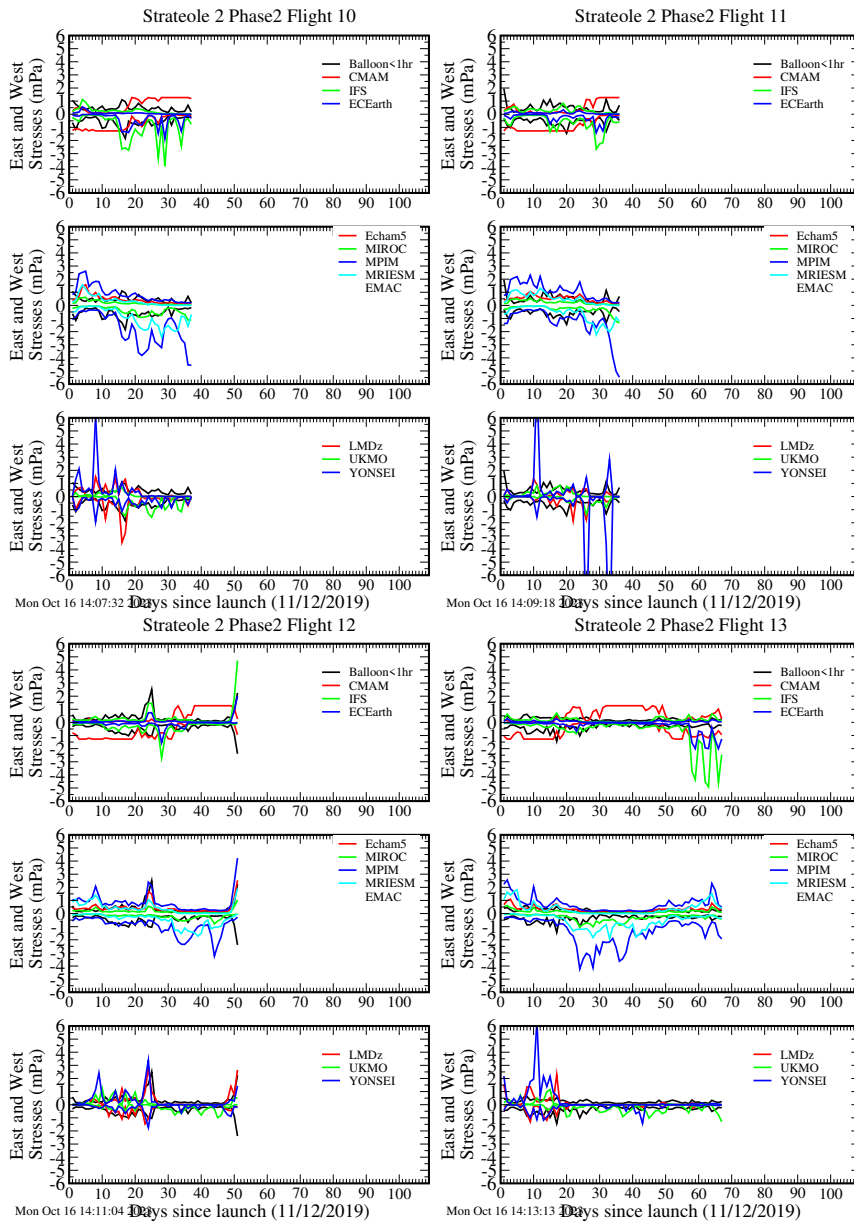


Supplementary: Phase 2 flights and models (continued)



754

Supplementary: Phase 2 flights and models (continued)



755

Supplementary: Phase 2 flights and models (continued)

